Glypican-1, -3, -5 (GPC1, GPC3, GPC5) and Hedgehog Pathway Expression in Oral Squamous Cell Carcinoma

Caroline B. Schlaepfer Sales, PhD, Vanessa S.N. Guimarães, MSc,*†*
Ludmila F. Valverde, PhD,† Rosane B. Dias, PhD,*† Raíza D. Freitas, MSc,*†*
*Leonardo de Oliveira Siquara da Rocha, BSc,† Malu Coelho de Miranda, BSc,**
Deise S. Vilas Bôas, PhD, Ivan M. Gonçalves Agra, PhD,* Jean N. dos Santos, PhD,**
and Clarissa A. Gurgel Rocha, PhD†*

Abstract: Proteoglycans are involved in tumor development and may regulate the Hedgehog (HH) pathway. This study aimed to investigate the gene and protein expression of glypican-1 (GPC1), -3 (GPC3), and -5 (GPC5) in oral squamous cell carcinoma (OSCC) and tumor-free lateral margins (TM) and their association with the HH pathway. Quantitative PCR was performed for *GPC1*, *GPC3*, *GPC5*, *SHH*, *PTCH1*, *SMO*, and *GLI1* genes in samples of OSCC (n = 31), TM (n = 12), and non-neoplastic oral mucosa (NNM) of healthy patients (n = 6), alongside an immunohistochemical evaluation of GPC1, GPC3, and GPC5 proteins and HH proteins SHH and glioma-associated oncogene homolog 1 (GLI1). Double staining for GPC3/SHH, GPC5/SHH, GPC3/tubulin [ac Lys40], GPC5/Tubulin [ac Lys40], and GPC5/GLI1 was also performed. Overexpression of *GPC1* and *GPC5* in tumor samples and underexpressed levels of *GPC3* gene transcripts were observed when compared with TM (standard sample). HH pathway mRNA aberrant expression in OSCC samples and a negative correlation between *GPC1* and *GPC5* at transcription levels were detected. GPC1 staining was rare in OSCC, but positive cells were found in NNM and TM. Otherwise positive immunostaining for GPC3 and GPC5 was observed in OSCCs, but not in NNM and TM. Blood vessels adjacent to tumor islands were positive for GPC1 and GPC5. Co-localization of GPC3-positive and GPC5-positive cells with SHH and Tubulin [ac Lys40] proteins was noted, as well as of GPC5 and GLI1. The absence of the GPC1 protein in neoplastic cells, underexpression of the *GPC3* gene, and co-localization of GPCs and HH proteins may indicate the maintenance of aberrant HH pathway activation in OSCC.

Key Words: oral cancer, real-time polymerase chain reaction, Immunohistochemistry, Hedgehog proteins, Heparan Sulfate proteoglycans

(*Appl Immunohistochem Mol Morphol* 2021;00:000–000)

Received for publication June 22, 2020; accepted December 28, 2020.
From the *Federal University of Bahia; and †Oswaldo Cruz Foundation, Gonçalo Moniz Institute, Laboratory of Pathology and Molecular Biology, Salvador, Brazil.
This study was financially supported by the National Council for Scientific and Technological Development (CNPq, Brazil) Grant numbers 446065 and 308276/2019-1.

The authors declare no conflict of interest.
Reprints: Clarissa A. Gurgel Rocha, PhD, Waldemar Falcão Street, 121, Candeal, Salvador/BA 40296-710, Brazil (e-mail: clarissa.gurgel@bahia.fiocruz.br).

Oral cancer is a serious public health concern as it represents the sixth most frequently occurring tumor worldwide, with oral squamous cell carcinoma (OSCC) corresponding to nearly 95% of diagnosed cases.[1] Approximately 500,000 new OSCC cases are reported annually, in addition to 7,000 disease-related deaths.[2]

Deregulation of embryonic signaling pathways, such as the Hedgehog (HH) pathway, can result in tumor development.[3–6] Reactivation of the HH pathway has been described in OSCC[7–9] and its precursor lesion, oral epithelial dysplasia.[10] HH pathway activity occurs in the primary cilia, a sensory organelle formed by a projection of the cellular plasma membrane composed of tubulin subunits.[11,12] In the absence of morphogens [sonic Hedgehog (SHH), Indian HH, or desert HH], the transmembrane receptor Patched 1 (PTCH1) is located within the primary cilium, promoting the suppression of smoothened (SMO) activity. After interacting with one of the HH ligands, PTCH1 receptor becomes translocated, resulting in consequent ciliary accumulation of SMO, which transduces the HH signal to the cytoplasm, culminating in nuclear migration of glioma-associated oncogene homolog 1 (GLI1) transcription factors and the activation of target genes involved in proliferation, survival, and HH pathway regulation.[11]

Glypicans (GPC) are proteoglycans from the family of proteins possessing heparan sulfate (HSPG), which interact with the plasma membrane through a glycosylphosphatidylinositol (GPI) anchor[13] and participate in morphogenesis through signaling pathway regulation, including the HH pathway.[14,15] In humans, six different types of GPCs have been identified,[16] most notably subtypes GPC1, GPC3, and GPC5. GPC1 and GPC3 are known to be negative regulators of the HH pathway. GPC1 acts by stabilizing the interaction between the morphogen and the inhibitor Hedgehog-interacting protein,[17] whereas GPC3 competes with the PTCH1 receptor for the SHH ligand, leading to increased morphogen degradation.[18] In turn, GPC5 contributes to the activation of this signaling cascade, as it acts to increase the interaction affinity between the morphogen and its receptor.[19]

Considering GPC1, GPC3, and GPC5 functions concerning HH pathway regulation described in pancreatic cancer,[13] liver cancer,[15,18] and rhabdomyosarcoma,[19] we endeavored to investigate the gene and protein expression profiles of GPC1, GPC3, and GPC5 in OSCC and tumor-free lateral margins (TM), and to examine any

TABLE 1. Clinical and Histologic Characteristics of 31 Cases of Oral Squamous Cell Carcinoma

Clinical Parameters	Total, n (%)
Sex	
Male	23 (74.18)
Female	8 (25.81)
Size	
T1-T2	15 (48.38)
T3-T4	15 (48.38)
Unclassified	1 (3.44)
Metastasis—lymph node	
N0	9 (29.03)
N1-N3	21 (67.55)
Unclassified	1 (3.22)
Metastasis—distance	
M0	31 (100.00)
Histologic gradation	
Well-differentiated	18 (58.06)
Moderately differentiated	7 (22.58)
Poorly differentiated	6 (19.36)
Anatomic site	
Tongue	13 (41.93)
Floor of the mouth	10 (32.25)
Retromolar region	5 (16.12)

associations between the studied GPCs and HH pathway component, as these relationships are not yet known in this tumor.

MATERIAL AND METHODS

Following approval by the Institutional Review Board of the Gonçalo Moniz Institute (Oswaldo Cruz Foundation, Salvador, Brazil), we investigated a series of 31 cases of OSCC and 12 of TM in patients admitted to a reference hospital for cancer treatment in the state of Bahia (Salvador). All patients included had not undergone any previous treatment for this tumor. For comparison purposes, we included 6 cases of non-neoplastic oral mucosa (NNM) from healthy patients, that is, nonsmokers who reported no alcohol consumption, obtained through the removal of unerupted third molars. All included patients provided informed written consent. The obtained specimens were sectioned into 2 fragments: 1 was kept in RNAlater (Invitrogen Corporation, USA) for 24 hours and was subsequently frozen in liquid nitrogen (−80°C), while the other was fixed in 10% neutral buffered formalin for histologic processing. Table 1 describes the clinical parameters and histologic classifications of the studied OSCC cases.

Gene Expression

Total RNA Isolation and Reverse Transcription (RT-PCR)

All frozen samples were homogenized using beads (L-Beader, Loccus Biotecnologia) and RNA was then extracted using the silica microcolumns of a Rneasy Plus Mini Kit (QIAGEN, Tokyo, Japan). RNA purity was evaluated by spectrophotometry (NanoDrop; Thermo Scientific, Wilmington, DC), whereas quantification was determined by fluorometry (QuBit, Life Technologies, USA). Genomic DNA was eliminated using DNAse I enzyme (Invitrogen Corporation, Carlsbad, CA). Reverse transcription was processed using the transcriptase enzyme SuperScript VILO cDNA Synthesis Kit (Invitrogen Corporation, Carlsbad, CA), and cDNA samples were stored at −20°C. All experiments were performed under DNAse/RNAse-free conditions.

Quantitative Polymerase Chain Reaction (qPCR)

GPC1 (Hs00892476_m1), *GPC3* (Hs00170471_m1), *GPC5* (Hs00270114_m1), *SHH* (Hs00179843_m1), *PTCH1* (Hs00181117_m1), *SMO* (Hs01090242_m1), and GLI1 (Hs01110766_m1) were evaluated by qPCR using TaqMan Gene Expression Assays. After evaluating a total of six (*18S, ACTB, B2M, GAPDH, HPRT1, UBC*) reference gene candidates, *ACTB* (Hs01060665_g1), *B2M* (Hs99999907_m1), and *UBC* (Hs01871556_s1) were selected for reaction normalization following analysis by Gene Expression Suite v.1.0.3 software (Applied Biosystems, Foster City, CA). A pool of 12 TM reference samples were used for calibration purposes.

All reactions were performed using an ABI ViiA7 Fast Real-Time PCR System (Applied Biosystems) in a 96-well plate at a total volume of 20 μL, with 8 μL of sample cDNA (20 ng/μL), 1 μL of Assay (Applied Biosystems), 10 μL of Taqman PCR Master Mix (Applied Biosystems), and 1 μL of RNAse-free water. The amplification protocol consisted of an initial cycle at 50°C for 2 minutes and at 95°C for 10 minutes, followed by 40 cycles at 95°C for 15 seconds and at 60°C for 1 minutes. After the amplification and dissociation run, relative quantification (RQ) values were obtained using Gene Expression Suite v.1.0.3 software (Applied Biosystems) following a comparative method for C_q ($2^{-\Delta\Delta CQ}$).[20] The genes were considered overexpressed if RQ ≥ 2, which means that the gene expression in OSCC and NNM was at least twice that in the pool of tumor margins. Similarly, the genes were considered underexpressed if RQ ≤ 0.5, which means that the gene expression in OSCC and NNM was half or less than half that in calibrator reactions.

Immunohistochemistry

Immunohistochemical analysis was performed on 26 OSCCs, 9 TMs, and 4 NNMs. All samples were submitted to immunostaining for GPC1 (Polyclonal; Santa Cruz, Dallas, TX), GPC3 (Clone 1312; Santa Cruz), GPC5 (Clone EPR6756 (B); Novus Biologicals, Centennial, CO) SHH (Clone 5H4; Novus Biologicals), GLI1 (Polyclonal; Novus Biologicals) antibodies, and Tubulin [ac Lys40] (Clone 6-11B-1, Novus Biologicals). Histological sections were deparaffinized in xylol and then rehydrated with alcohol. To reveal antigenic epitopes, sections were submitted to antigenic recovery under humidity for 45 minutes. Next, endogenous peroxidase blocking (Peroxidase Blocking Solution; Dako, Carpinteria, CA) and tissue protein blocking (Protein Blocking Solution; Dako) were performed. Primary antibodies were incubated overnight at 4°C, after which HRP link and HRP enzyme reagents (Advance, Dako Corporation) were applied. For the anti-GPC1 antibody, the LSAB K0610 detection system (Dako Corporation) was used. Reactions were revealed by 3,3-diaminobenzidine (Dako Corporation) and counterstained using Harris hematoxylin. For negative controls, each primary antibody was replaced by normal serum of the same isotype.

Section images were captured using an Olympus VS110 Virtual Slide Microscope Scanning System (Olympus Corporation, Tokyo, Japan) and displayed on a high-resolution monitor using Olyvia 2.3 Software (Olympus Corporation).

For protein analysis, antigen localization was also taken into account, whether occurring in the membrane and/or cytoplasm, in the tumor cells/epithelium, or the stroma/lamina propria. Accordingly, samples were then categorized based on the following semiquantification criteria: (−) negative, score (0) <5% of positively immunostained cells; (1+) between 6% and 25%; (2+) 26% to 50%; (3+) 51% to 75%; (4+) >75% of positively stained cells.

Co-localization of GPC3/SHH, GPC5/SHH, GPC3/Tubulin [ac Lys40], GPC5/Tubulin [ac Lys40], and GPC5/GLI1 was identified using the EnVision G|2 Doublestain and Advance polymeric amplification systems (Dako Corporation). Reactions were visualized using Permanent Red Working Solution (Dako Corporation) and Vina Green (Biocare Medical) chromogens, whereas 3,3-diaminobenzidine (Dako) and Permanent Red Working Solution (Dako Corporation) were used for GLI1/GPC5.

Statistical Analysis

All statistical analyses were performed using GraphPad Prism 8 (GraphPad Software Inc., San Diego, CA). The Fisher exact test was used to compare proportions, whereas the Mann-Whitney *U* test and unpaired *t* test were utilized to compare 2 independent groups. Kruskal-Wallis test and the Dunn posttest were used to compare 3 or more groups, and the Spearman rank correlation coefficient was used to evaluate correlations between 2 variables. When $P < 5\%$ it was considered statistically significant.

RESULTS

Gene Expression Profile of GPCS and HH Genes

GPC1 and *GPC5* mRNA were identified in 26 (83%) and 15 (48%) OSCC cases, respectively, at transcription levels 2× and 7× greater than TMs. By contrast, *GPC3* was found to be underexpressed (n = 22, 71%, mean RQ = 0.16) in OSCC. Detected levels of GPC transcription are shown in Figure 1A and Table 2. All evaluated HH pathway transcripts were found to be overexpressed (RQ values are shown in Table 2),

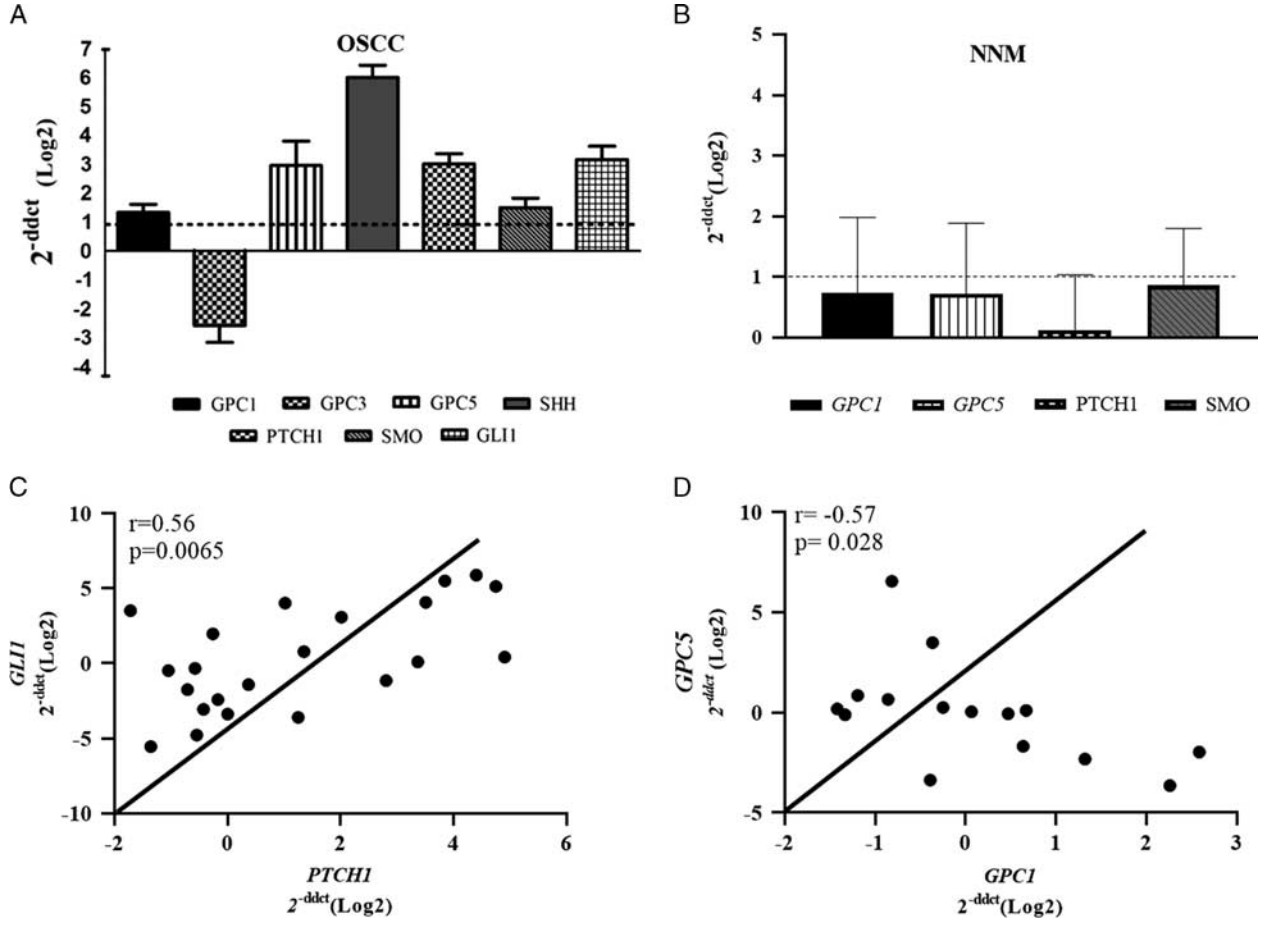

FIGURE 1. Gene expression profile of *GPC1*, *GPC3*, *GPC5*, *SHH*, *PTCH1*, *SMO*, and *GLI1*. A, Logged relative quantification (RQ) of *GPC1*, *GPC3*, *GPC5*, *SHH*, *PTCH1*, *SMO*, and *GLI1* genes in oral squamous cell carcinoma (OSCC) cases. B, Logged relative quantification (RQ) of *GPC1*, *GPC5*, *PTCH1*, and *SMO* genes in non-neoplastic oral mucosa (NNM) cases. C, Correlation between *PTCH1* and *GLI1* genes. D, Correlation between *GPC1* and *GPC5* genes.

TABLE 2. Expression of *SHH*, *PTCH1*, *SMO*, *GLI1*, *GPC1*, *GPC3*, and *GPC5* Genes in 31 Cases of Oral Squamous Cell Carcinoma

Target	n (%)	Average $C_t \pm$ SD	Average $\Delta C_t \pm$ SD	$\Delta\Delta C_t$	Mean Fold Change Relative to Controls	Mean Fold Change (Log2)
GPC1	26 (83.87)	28.39 ± 2.47	2.59 ± 1.75	−1.230	2.51 (0.30-9.14)	1.33 (−1.71 to 3.19)
GPC3	22 (70.96)	28.83 ± 2.11	3.84 ± 2.48	−1.473	0.16 (0.007-0.95)	−2.58 (0.007 to −0.06)
GPC5	15 (48.38)	33.49 ± 2.15	8.34 ± 2.74	−0.481	7.72 (0.08-93.92)	2.94 (−3.56 to 6.55)
SHH	5 (16.13)	33.99 ± 1.27	4.92 ± 2.06	−4.219	63.98 (4.1-132.9)	5.99 (2.03-7.05)
PTCH1	25 (80.64)	30.46 ± 2.31	4.09 ± 2.64	−0.237	8.03 (0.30-42.33)	3.00 (−1.71 to 5.40)
SMO	26 (83.87)	29.31 ± 2.28	2.80 ± 1.81	−0.513	2.82 (0.13-16.74)	1.48 (−2.88 to 4.06)
GLI1	23 (74.19)	30.98 ± 2.60	8.39 ± 3.51	−0.095	8.90 (0.02-59.30)	3.15 (−5.57 to 5.89)

demonstrating the activity of this signaling cascade in the present OSCC case series (Fig. 1A).

In tumor samples, correlation between the investigated genes was evaluated. A positive correlation was found between *PTCH1* and *GLI1* genes ($r = 0.56$, $P = 0.00065$) (Fig. 1C), and a negative correlation was observed between *GPC1* and *GPC5* ($r = -0.57$, $P = 0.002$) (Fig. 1D). Transcript levels of *GPC1*, *GPC3*, *GPC5*, *SHH*, *PTCH1*, *SMO*, and *GLI1* were found to be similar concerning the clinical and morphological parameters evaluated (Table 3).

For comparative purposes, the expression profiles of these same genes were also analyzed in samples of oral mucosa from healthy patients. No *SHH* transcripts were detected in any of the NNM samples, nor was *GPC3* mRNA. All other investigated genes were positively identified in all NNM samples, with expression levels similar to what was seen in TMs (*GPC1*, mean RQ = 1.67/log2 = 0.73; *GPC5*, RQ = 1.65/log2 = 0.74; *PTCH1*, mean RQ = 1.09/log2 = 0.12; *SMO*, mean RQ = 1.82/log2 = 0.86) (Fig. 1B).

Immunostaining for GPC1, GPC3, and GPC5

Concerning immunostaining for GPC1, this protein was found to be localized in tumor cells in 12 (46.15%) tumors, yet 8 cases (66.66%) presented immunostaining in <5% of all cells (ie, score 0) (Table 4). Positive cells were particularly seen in the centers of tumor islands. In tumor stroma, some blood vessels exhibited positivity for GPC1. In NNM and TM cases, the GPC1 protein was observed in the membranes and cytoplasm of epithelial cells, especially the spinal stratum (Fig. 2), scored predominantly as 3+ (n = 3; 75%) and 4+ (n = 5; 55.56%), respectively.

The GPC3 protein was localized in tumor cells, mainly in the peripheral areas around tumor islands and at the invasion front, presenting both membrane and cytoplasmic immunostaining. Of the 23 (88.46%) OSCCs positive for GPC3, 11 (42.30%) presented 5% or fewer immunostained cells (score 0), followed by a score of 1+ (n = 5, 19.23%) (Table 4). No immunoreactivity was detected for GPC3 in NNM (n = 4; 0%) or TM (n = 9; 0%) (Fig. 2).

In OSCC, 13 (50%) samples presented cytoplasmic immunostaining for GPC5 in tumoral cells, with a predominant score of 1+ (n = 5; 38.46%) (Table 4). Positivity was observed in tumor stroma, with immunostaining evident in endothelial cells and fibroblasts. GPC5 was not detected in NNM (n = 4; 100%) and, in TMs, basal and spiny strata cells exhibited discrete cytoplasmic staining, predominantly with a score of 1+ (n = 2; 22.22%) (Fig. 2).

GPCS and HH Component Immunostaining Relationship in OSCC

Initially, the SHH and GLI1 immunostaining profile was characterized, and both proteins were positive in 23 OSCC cases (88.46%), scored predominantly 4+ (SHH = 61.53% and GLI1 = 53.85%). With regard to SHH, cytoplasmic immunoreactivity was observed, whereas GLI1 presence was detected on the nucleus and cytoplasm of tumor cells, and on stroma cells (Fig. 3).

Then to evaluate the interactions between GPCs and HH pathway components, double staining for GPC3/SHH, GPC5/SHH, GPC3/Tubulin [ac Lys40], GPC5/Tubulin [ac Lys40], and GPC5/GLI1 was performed (Fig. 4). The co-localization of GPC3/SHH was exclusively visualized in the cytoplasm of

TABLE 3. Levels of *GPC1*, *GPC3*, *GPC5*, *SHH*, *PTCH1*, *SMO*, and GLI1 Were Found to be Similar With Regard to the Clinical and Morphological Parameters Evaluated

		GPC1		*GPC3*		*GPC5*		*SHH**		*PTCH1*		*SMO*		*GLI1*	
Parameters	**Total**	**Median**	***P***	**Median**	***P***	**Median**	***P***	**OSCC + (%)**	***P***	**Median**	***P***	**Median**	***P***	**Median**	***P***
Size															
T1-T2	15	1.59	0.34	0.046	0.44	0.96	0.81	3 (9.67)	0.63	0.83	0.31	0.51	0.49	0.48	0.45
T3-T4	15	0.80		0.044		0.67		2 (6.45)		2.52		1.81		0.65	
Lymph node involvement															
N0	9	0.80	0.62	0.043	0.69	0.94	0.40	3 (9.67)	1.00	0.74	0.10	0.40	**0.01**	2.02	0.07
N1-N3	21	1.55		0.046		1.13		2 (6.45)		2.46		2.65		0.82	
Histologic grade															
Well-differentiated	18	0.80		0.046		1.10		3 (9.67)		2.20		1.46	0.56	0.79	
Moderately differentiated	7	1.94	0.35	0.044	0.89	0.09	0.05	2 (6.45)	0.63	0.68	0.12	0.49		0.30	0.28
Poorly differentiated	6	4.23		0.16		0.96		—	—	10.16		3.25		4.03	

Bold value indicates statistical significance ($P < 0.05$).
*The Fisher exact test.

TABLE 4. Distribution of Semiquantification Scoring for GPC1, GPC3, GPC5, SHH, and GLI1 Proteins in Tumor Cells of OSCC Cases

	GPC1	GPC3	GPC5	SHH	GLI1
Score	Total (%)	Total (%)	Total (%)	Total (%)	Total (%)
Negative	14 (53.85)	3 (11.53)	13 (50)	3 (11.53)	3 (11.53)
0 (< 5%)	8 (30.77)	11 (42.30)	5 (19.23)	0	0
1+	0	5 (19.23)	5 (19.23)	2 (7.69)	1 (3.84)
2+	3 (11.54)	2 (7.69)	2 (7.69)	0	1 (3.84)
3+	1 (3.84)	3 (11.56)	0	5 (19.23)	7 (26.92)
4+	0	2 (7.69)	1 (3.85)	16 (61.53)	14 (53.85)

tumor cells, while GPC5/SHH was present in the tumor cells and tumor stroma. We also detected the expression of Tubulin [ac Lys40] in GPC3-positive and GPC5-positive cells. In addition, GLI1 transcription factor was found in cells positive for GPC5 within the tumor cells and stroma of OSCCs.

DISCUSSION

GPC proteins may be involved in various aspects of tumorigenesis such as cancer cell growth, progression,[13,14] and modulation of HH cascade.[15,17–19] In this study, we observed the presence of GPC3 and GPC5 in tumor cells and their absence in normal samples, which indicate that they are partaking as oncoproteins, as described in hepatocarcinoma and rhabdomyosarcoma studies.[15,19] Furthermore, the absence of the GPC1 protein, which plays a role in attenuating HH signaling, concomitant to GPC3 and GPC5 co-localization with HH proteins suggest that GPC1, GPC3, and GPC5 may participate in HH pathway regulation in the context of OSCC.

GPCs have been well characterized in some malignant tumors, as is the case of GPC1 in pancreatic cancer,[21] GPC3 in hepatocellular carcinoma,[22] and GPC5 in rhabdomyosarcoma.[19] These proteins are known to exercise important roles in the biological processes of these types of tumors, acting as both oncogenic and tumor suppressor proteins, in addition

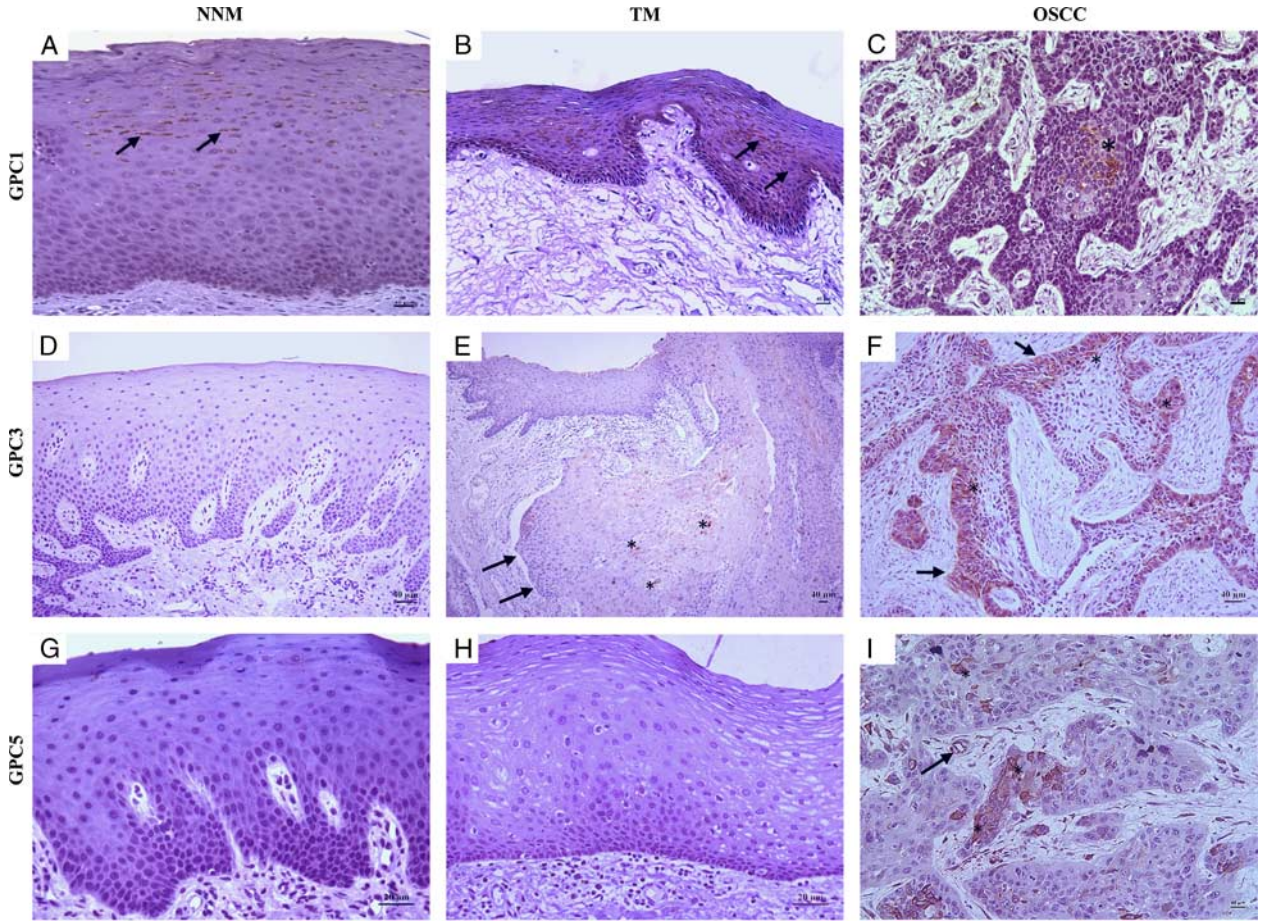

FIGURE 2. Immunostaining for GPC1, GPC3, and GPC5 in the non-neoplastic oral mucosa (NNM), tumor-free lateral margins (TM), and oral squamous cell carcinoma (OSCC). A–C, GPC1: (A) positive cells, especially in the spinal stratum (arrows), in NNM and (B) TM. C, Positive cells (*) in OSCC with a corresponding score of 0. D–F, GPC3: (D) negative score in NNM. E, TM with negative score and invasion front (arrows) showing GPC3-positive cells (*). F, Membrane (*) and cytoplasmic (**) immunostaining in tumor cells, especially along the periphery of tumor islands (arrows) with a score of 1+. G–I, GPC5: (G) NNM with negative score. H, Positive score of 1+ in TM. I, Cytoplasmic (*) immunostaining in tumor cells with a score of 1+; positivity in tumor stroma vessels (arrow).

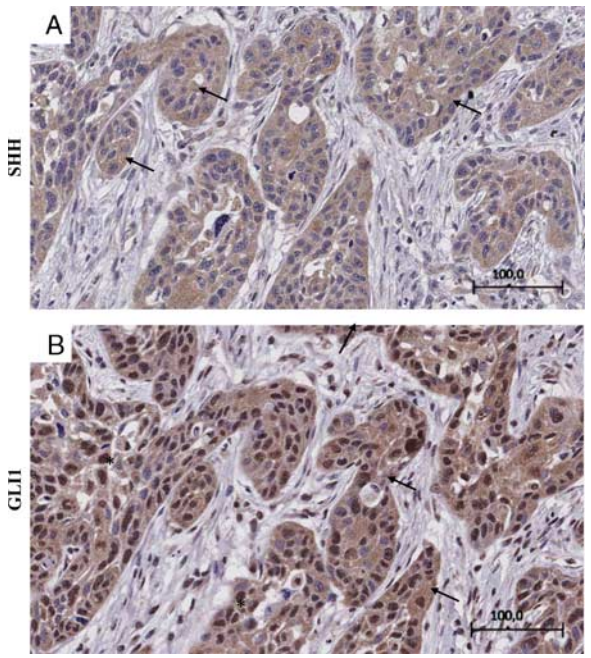

FIGURE 3. Immunostaining for SHH and GLI1 in oral squamous cell carcinoma (OSCC). A, Cytoplasmic immunostaining in tumor cells for SHH with 4+ score (arrows). B, Nuclear (*) and cytoplasmic (arrows) immunostaining in tumor cells and some stroma cells. full color online

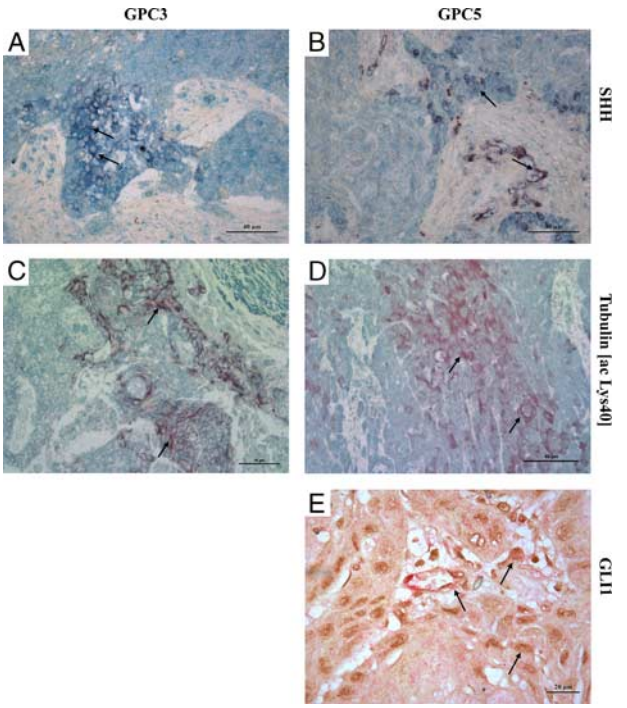

FIGURE 4. Double-staining for GPC3 and GPC5 with Hedgehog (HH) pathway components (SHH, Tubulin [ac Lys40], and GLI1) in oral squamous cell carcinoma (OSCC). A, Cytoplasmic co-localization of GPC3 (Red Permanent)/SHH (Vina Green) in tumor cells and (B) co-localization of GPC5 (Red Permanent)/SHH (Vina Green) in tumor cells and stroma. C, Co-localization of GPC3 (Vina Green) and Tubulin [ac Lys40] (Red Permanent) in tumor cells. D, GPC5 (Vina Green) and Tubulin [ac Lys40] (Red Permanent) in tumor cells. E, Co-localization of GPC5 (Red Permanent) in the cytoplasm and GLI1 (DAB) in the nucleus in tumor cells and stroma. Arrows indicate the co-localizations cited above. full color online

to participating in HH pathway regulation.[15,18] This notwithstanding, a review of the scientific literature found no reports that specifically evaluated the influence of GPCs on HH signaling in the context of OSCC.

Our initial evaluation of HH pathway activity verified the deregulation of this signaling pathway in the OSCC cases studied, as confirmed by the overexpression of *PTCH1*, *SMO*, and *GLI1* genes, and high levels of SHH and GLI1 protein. Although *SHH* transcripts were infrequently found, elevated levels were detected when expressed. While equivalent concentrations of ligands and receptors are an expected finding in signaling pathways,[23] the HH pathway is an exception,[24] as PTCH1 is a target gene for GLI transcription factors.[25]

While the present results highlight the overexpression of *GPC1* and *GPC5* genes in OSCC, blood vessels adjacent to tumor islands were found to be positive for GPC1 and GPC5, suggesting the potential participation of these proteins in the regulation of angiogenesis in OSCC. Despite the well-defined relationship between GPC1 and angiogenesis in other tumors, such as pancreatic and esophageal squamous cell carcinoma,[21,26] no studies have described any involvement of GPC5 in the development of new vessels. It is noteworthy that the present results demonstrate GPC5/GLI co-localization. A recent report confirmed that blood vessels expressing the GLI1 protein were also positive for CD105, which has been previously linked to tumor angiogenesis.[27]

At the transcriptional level, we noted an underexpression of *GPC3* in OSCC, despite clear evidence of this protein's localization in tumoral tissues. In melanoma, Nakatsura et al[28] also reported a lack of correlation between levels of *GPC3* mRNA and protein expression. An explanation for this may be that when GPC3 is internalized as an SHH ligand, the morphogen becomes degraded,[18] in contrast to other GPCs, which are recycled and then return to the plasma membrane.[29] The present results corroborate this aspect, as evidenced by the concomitant presence of GPC3/SHH in the cytoplasm and GPC3/Tubulin [ac Lys40] in tumor cells, which reinforces the notion of HH pathway regulation occurring through GPC3 in OSCC. Nonetheless, decreased expression of GPC1 protein was seen in tumor cells, even though this proteoglycan is known to aid in the interaction between the SHH ligand and the Hedgehog-interacting protein inhibitor, which thereby promotes HH pathway inactivation.[15] Accordingly, the absence of GPC1 protein expression in neoplastic cells may contribute to the maintenance of HH pathway activity in OSCC.

The transcriptional and protein levels of GPC5 in the OSCCs studied, and the co-localization of proteins GPC5/SHH, Tubulin [ac Lys40]/GPC5, and GPC5/GLI1, indicate that this molecule may aid in the activation of the HH pathway in OSCC by enhancing the affinity between HH ligands and their receptors,[15,19] or even by aiding in

the endocytosis of SHH,[25,30] which emphasizes the need for further investigation into the mechanisms involved in HH signaling internalization in this tumor type.

Moreover, the present results also demonstrate that OSCC cases with the greatest degree of tumor cell immunostaining for the GPC3 protein were negative for GPC5 in this same tumor compartment. On the contrary, GPC5 was found to be present in tumor stroma in the absence of GPC3. Furthermore, a negative correlation was observed between *GPC1* and *GPC5* at transcription levels. In light of these findings, taking into consideration that GPC1 and GPC3 have been shown to attenuate HH pathway activity[15,17,18] and that GPC5 is also a positive regulator,[19] this further reinforces the role of these proteoglycans as potential regulators of the HH pathway in OSCC.

Also, the accumulation of GPC3 and GPC5 proteins in OSCC along with the absence of these GPCs in nontumoral tissues (NNM and TM), as previously observed in hepatocellular carcinoma,[22] melanoma,[28] and rhabdomyosarcoma,[19] appear to be indicative of an oncogenic role played by these GPCs in OSCC, an aspect that warrants further investigation.

In conclusion, the present study introduced data related to the expression of GPC1, GPC3, and GPC5 in OSCC and TMs, and the correlation between these proteoglycans and HH cascade. The presence of GPC1 and GPC5 proteins in tumor stroma, notably in blood vessels, calls for additional research regarding the participation of these proteoglycans in the OSCC angiogenesis.

ACKNOWLEDGMENTS

The authors thank Andris K. Walter for providing English translation and consulting services.

REFERENCES

1. Miranda-Filho A, Bray F. Global patterns and trends in cancers of the lip, tongue and mouth. *Oral Oncol*. 2020;102:1–8.
2. Bray F, Ferlay J, Soerjomataram I, et al. Global cancer statistics 2018: GLOBOCAN estimates of incidence and mortality worldwide for 36 cancers in 185 countries. *CA Cancer J Clin*. 2018;68:394–424.
3. Thayer SP, Di Magliano MP, Heiser PW, et al. Hedgehog is an early and late mediator of pancreatic cancer tumorigenesis. *Nature*. 2003;425:851–856.
4. Skoda AM, Simovic D, Karin V, et al. The role of the Hedgehog signaling pathway in cancer: a comprehensive review. *Bosn J basic Med Sci*. 2018;18:8–20.
5. Wu F, Zhang Y, Sun B, et al. Hedgehog signaling: from basic biology to cancer therapy. *Cell Chem Biol*. 2017;24:252–280.
6. Agrawal V, Kim DY, Kwon YG. Hhip regulates tumor-stroma-mediated upregulation of tumor angiogenesis. *Exp Mol Med*. 2017;49:1–8.
7. Cavicchioli Buim ME, Gurgel CAS, Gonçalves Ramos EA, et al. Activation of sonic hedgehog signaling in oral squamous cell carcinomas: a preliminary study. *Hum Pathol*. 2011;42:1484–1490.
8. Leovic D, Sabol M, Ozretic P, et al. Hh-Gli signaling pathway activity in oral and oropharyngeal squamous cell carcinoma. *Head Neck*. 2012;34:104–112.
9. Valverde LF, Pereira TA, Dias RB, et al. Macrophages and endothelial cells orchestrate tumor-associated angiogenesis in oral cancer via hedgehog pathway activation. *Tumor Biol*. 2016;37:9233–9341.
10. Dias RB, Valverde LF, Sales CBS, et al. Enhanced expression of hedgehog pathway proteins in oral epithelial dysplasia. *Appl Immunohistochem Mol Morphol*. 2016;24:596–602.
11. Hassounah NB, Bunch TA, McDermott KM. Molecular pathways: the role of primary cilia in cancer progression and therapeutics with a focus on hedgehog signaling. *Clin Cancer Res*. 2012;18:2429–2435.
12. Pedersen LB, Mogensen JB, Christensen ST. Endocytic control of cellular signaling at the primary cilium. *Trends Biochem Sci*. 2016;41:784–797.
13. Li N, Gao W, Zhang YF, et al. Glypicans as cancer therapeutic targets. *Trends in Cancer*. 2018;4:741–754.
14. Fico A, Maina F, Dono R. Fine-tuning of cell signaling by glypicans. *Cell Mol Life Sci*. 2011;68:923–929.
15. Filmus J, Capurro M. The role of glypicans in Hedgehog signaling. *Matrix Biol*. 2014;35:248–252.
16. Fransson LÅ. Glypicans. *Int J Biochem Cell Biol*. 2003;35:125–129.
17. Wilson NH, Stoeckli ET. Sonic Hedgehog regulates its own receptor on postcrossing commissural axons in a glypican1-dependent manner. *Neuron*. 2013;79:478–491.
18. Capurro MI, Xu P, Shi W, et al. Glypican-3 inhibits Hedgehog signaling during development by competing with patched for Hedgehog binding. *Dev Cell*. 2008;14:700–711.
19. Li F, Shi W, Capurro M, et al. Glypican-5 stimulates rhabdomyosarcoma cell proliferation by activating Hedgehog signaling. *J Cell Biol*. 2011;192:691–704.
20. Livak KJ, Schmittgen TD. Analysis of relative gene expression data using real-time quantitative PCR and the 2(-Delta Delta C(T)) Method. *Methods*. 2001;25:402–408.
21. Aikawa T, Whipple CA, Lopez ME, et al. Glypican-1 modulates the angiogenic and metastatic potential of human and mouse cancer cells. *J Clin Invest*. 2008;118:89–99.
22. Shimizu Y, Suzuki T, Yoshikawa T, et al. Next-generation cancer immunotherapy targeting glypican-3. *Front Oncol*. 2019;9:1–10.
23. Rogers KW, Schier AF. Morphogen gradients: from generation to interpretation. *Annu Rev Cell Dev Biol*. 2011;27:377–407.
24. Casali A, Struhl G. Reading the hedgehog morphogen gradient by measuring the ratio of bound to unbound patched protein. *Nature*. 2004;431:76–80.
25. Gorojankina T. Hedgehog signaling pathway: a novel model and molecular mechanisms of signal transduction. *Cell Mol Life Sci*. 2016;73:1317–1332.
26. Harada E, Serada S, Fujimoto M, et al. Glypican-1 targeted antibody-based therapy induces preclinical antitumor activity against esophageal squamous cell carcinoma. *Oncotarget*. 2017;8:24741–24752.
27. Deliu IC, Neagoe CD, Beznă M, et al. Correlations between endothelial cell markers CD31, CD34 and CD105 in colorectal carcinoma. *Rom J Morphol Embryol*. 2016;57:1025–1030.
28. Nakatsura T, Kageshita T, Ito S, et al. Identification of Glypican-3 as a Novel Tumor Marker for Melanoma. *Clin Cancer Res*. 2004;10:6612–6621.
29. Christianson HC, Belting M. Heparan sulfate proteoglycan as a cell-surface endocytosis receptor. *Matrix Biol*. 2014;35:51–55.
30. Witt RM, Hecht ML, Pazyra-Murphy MF, et al. Heparan sulfate proteoglycans containing a glypican 5 core and 2-O-sulfo-iduronic acid function as sonic hedgehog co-receptors to promote proliferation. *J Biol Chem*. 2013;288:26275–26288.